

A Synthetic Generator of Myocardial Blood-Oxygen-Level-Dependent MRI Timeseries with Structural Sparse Decomposition Modeling

Cristian Rusu¹, Rohan Dharmakumar^{2,3}, and Sotirios A. Tsaftaris^{1,4}

¹IMT Institute for Advanced Studies Lucca, Lucca, Italy; ²Biomedical Imaging Research Institute, Cedars-Sinai Medical Center, Los Angeles, CA, United States; ³Medicine, University of California, Los Angeles, CA, United States; ⁴Electrical Engineering and Computer Science, Northwestern University, Evanston, IL, United States

Introduction: Recently a new contrast and stress-free approach for detecting myocardial ischemia at rest was demonstrated using Cardiac Phase resolved Blood Oxygen-Level-Dependent (CP-BOLD) MRI¹. This method has the potential to open the road to repeatable, truly non-invasive diagnosis of ischemic heart disease, primarily in detecting and triaging patients experiencing acute coronary syndromes (ACS) and particularly in cases of non ST elevation myocardial infarction. To identify the disease, CP-BOLD relies on the observation that myocardial signal intensity varies as a function of cardiac phase: in healthy conditions it is maximal in systole and minimal in diastole, but in disease scenarios this pattern changes due to perturbations in blood volume and oxygenation (affected by the coronary narrowing).¹ However, visualizing and quantifying such changes requires significant post-processing (segmentation and registration) to obtain the timeseries and detection algorithms that can identify differences in timeseries originating from ischemic parts of the myocardium. Unfortunately due to the lack of precise registration methods only a few images of the cine acquisition are used and segmental analysis is employed. Thus, specificity is potentially lost in characterizing the extent of ischemia.²

Purpose: New methods that can utilize the whole timeseries in defining biomarkers should bring the specificity of CP-BOLD to the pixel level and accelerate clinical translation, but the development of such methods is delayed by the lack of appropriate test data. We hypothesized that sparse decomposition with dictionary algorithms can learn and generate synthetic data (timeseries) on request.

Methods: Imaging Studies: Flow and motion compensated 2D short-axis CP-BOLD³ were acquired along the mid ventricle in 10 canines at baseline and under a severe LAD stenosis (in excess of $\approx 90\%$ flow reduction) as verified by Doppler flow velocities. Imaging studies were performed on a 1.5T Espree, (Siemens Healthcare). Scan parameters were: spatial resolution= $1.2 \times 1.2 \times 8 \text{ mm}^3$, flip-angle= 70° and $T_R/T_E = 6.2/3.1 \text{ ms}$. **Image Processing:** End-systolic (ES) and end-diastolic (ED) images were identified, myocardial borders were traced (in all phases) and segmented in 24 radially consecutive segments (dividing in 4 each segment of the AHA model), obtaining for each segment a 1D CP-resolved timeseries. All timeseries were interpolated to have a fixed length of 28 and arranged (from all studies, subjects and segments) column-wise in a matrix Y , 28×480 . Of those timeseries 80 were identified, based on the visual evaluation of late enhancement imaging, as belonging to ischemic myocardium (affected by LAD stenosis) and 400 otherwise (baseline or remote). A composite approach was used to find a dictionary D and sparse representations X of sparsity s , such that $Y \approx DX$, i.e., a column of Y is a linear combination of columns of D (termed atoms) with coefficients of X . To account for the circular structure in the baseline data (since most timeseries follow a similar cyclic pattern), D was split into two components and D , X (of sparsity 4) were found with specialized algorithms: a circulant one accounting for cyclic structure permitting 1 out of 4 cyclic shifts,⁴ and a generic one⁵ allowing for 3 atoms out of total 6. The approximation $Y \approx DX$ decomposes the input space in a collection of subspaces of much lower dimension (s). On the basis of this approximation, we fitted Gaussian Mixture Models (GMMs) on the distribution of the coefficients of each subspace of X . A similar approach is used to learn an ischemic model although no structure is imposed, designing 7 general atoms⁵ with sparsity 6. The outcome for each conditional state is a model composed of D , the statistical sub-models extracted from each utilized subspace and control parameters. These models are used to create synthetic timeseries directly, by drawing coefficients from the GMMs of each sub-model, and using them as weights to linearly combine the atoms of D involved in each individual subspace. Also, if required, noise is added to each timeseries to resemble different acquisition scenarios for future testing. **Statistical validation:** To validate the accuracy of the synthetic timeseries we learn 2 class Support Vector Machines on real timeseries (480 total: 80 ischemic, 400 baseline) and test on 100 instances of 480 synthetic timeseries (of the same composition) and vice versa, and measure agreement based on the known status (ischemic or baseline). T-tests are used to show the average performance (of agreement) between the previous classifiers compared to the cross-validation performance on real data (training on 9 canines and testing on the one left out).

Results: Fig. 1 shows the atoms obtained with the proposed decomposition. The cyclic atom, which we term the characteristic CP-BOLD curve, relates CP-BOLD signal intensity as a function of cardiac phase: at $\approx 33\%$ of the nominal cardiac cycle a high value is present. Interestingly using one of the four cyclic shifts to approximate a timeseries the model accounts for 60% of the energy, indicating a strong cyclic structure in the data. Linear combinations of a single cyclic shift of the atom and 3 (out of 6) general atoms encode well the input baseline timeseries. When the coefficients of the approximation are modeled with GMMs, real and synthetic data (obtained by sampling from the GMMs and combining the atoms) look visually similar (see Fig. 2). Quantitatively, validation shows that on average when training on real data, but testing on synthetic, in $84 \pm 0.7\%$ of the cases the correct originating status of the timeseries is found. In the reverse case, training on synthetic and testing on real, this number is $85 \pm 0.5\%$. Cross validation performance was $83 \pm 6\%$, and all t-tests showed statistical insignificance to differences in average accuracy ($p > 0.5$).

Discussion: With the proposed framework, we identify at baseline conditions a curve that strengthens evidence that the BOLD effect varies throughout the cardiac cycle. We find that all baseline CP-BOLD timeseries follow this curve's properties, but could shift due to differences in cardiac cycle among subjects. The proposed decomposition provides access to this curve and its shifts and as such can be used to accurately model, in a parameter free fashion, and represent the data, as our validation showed. By changing parameters of the added noise and mean, and modifying the shape of the cyclic atom, acquisition scenarios such as different flip angles, magnet strengths (e.g., 1.5T or 3T) can be simulated.

Conclusion: The presented method can generate realistic CP-BOLD timeseries, by representing the data efficiently, taking advantage of a unique sparse decomposition framework to produce parsimonious models that are easy to control and sample. Such timeseries can be integrated directly with image generators,⁶ to create 4D synthetic CP-BOLD datasets. Its application towards the development of improved ischemia detection methods and also the simulation of different imaging scenarios when designing CP-BOLD acquisitions and experiments will accelerate the clinical translation of this truly non-invasive and repeatable method for assessment of myocardial ischemia.

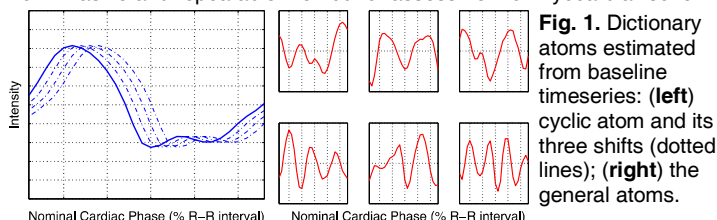


Fig. 1. Dictionary atoms estimated from baseline timeseries: (left) cyclic atom and its three shifts (dotted lines); (right) the general atoms.

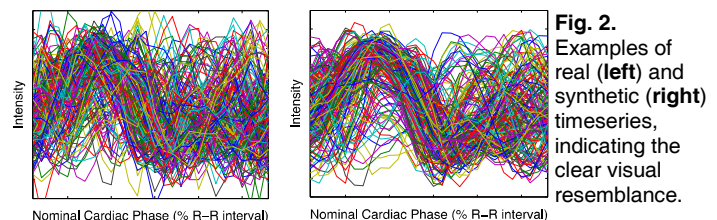


Fig. 2. Examples of real (left) and synthetic (right) timeseries, indicating the clear visual resemblance.

References: (1) Tsaftaris et al, *Circ Card. Img* 6(2):311-9 2013; (2) Tsaftaris et al, *JMRI* 35(6):1338-48 2012; (3) Zhou et al, *JMRI* 31(4):863-71 2010; (4) Rusu, Dumitrescu, Tsaftaris, *IEEE SPL* 2014; (5) Aharon et al, *IEEE TSP*, 54(11):4311-22 2006; (6) Prakosa et al, *IEEE TMI* 32(1):99-109 2013.